

# REPORT DOCUMENTATION PAGE

Form Approved  
OMB No. 0704-0188

Public reporting burden for this collection of information is estimated to average 1 hour per response, including the time for reviewing instructions, searching existing data sources, gathering and maintaining the data needed, and completing and reviewing this collection of information. Send comments regarding this burden estimate or any other aspect of this collection of information, including suggestions for reducing this burden to Department of Defense, Washington Headquarters Services, Directorate for Information Operations and Reports (0704-0188), 1215 Jefferson Davis Highway, Suite 1204, Arlington, VA 22202-4302. Respondents should be aware that notwithstanding any other provision of law, no person shall be subject to any penalty for failing to comply with a collection of information if it does not display a currently valid OMB control number. PLEASE DO NOT RETURN YOUR FORM TO THE ABOVE ADDRESS.

1. REPORT DATE (DD-MM-YYYY)

2. REPORT TYPE

Technical Papers

3. DATES COVERED (From - To)

4. TITLE AND SUBTITLE

5a. CONTRACT NUMBER

5b. GRANT NUMBER

5c. PROGRAM ELEMENT NUMBER

6. AUTHOR(S)

5d. PROJECT NUMBER

2303

5e. TASK NUMBER

m1A3

5f. WORK UNIT NUMBER

7. PERFORMING ORGANIZATION NAME(S) AND ADDRESS(ES)

Air Force Research Laboratory (AFMC)  
AFRL/PRS  
5 Pollux Drive  
Edwards AFB CA 93524-7048

8. PERFORMING ORGANIZATION  
REPORT

9. SPONSORING / MONITORING AGENCY NAME(S) AND ADDRESS(ES)

Air Force Research Laboratory (AFMC)  
AFRL/PRS  
5 Pollux Drive  
Edwards AFB CA 93524-7048

10. SPONSOR/MONITOR'S  
ACRONYM(S)

11. SPONSOR/MONITOR'S  
NUMBER(S)

12. DISTRIBUTION / AVAILABILITY STATEMENT

Approved for public release; distribution unlimited.

13. SUPPLEMENTARY NOTES

14. ABSTRACT

20030110 073

15. SUBJECT TERMS

16. SECURITY CLASSIFICATION OF:

17. LIMITATION  
OF ABSTRACT

18. NUMBER  
OF PAGES

19a. NAME OF RESPONSIBLE  
PERSON

Leilani Richardson

a. REPORT

b. ABSTRACT

c. THIS PAGE

Unclassified

Unclassified

Unclassified

A

19b. TELEPHONE NUMBER

(include area code)  
(661) 275-5015

Standard Form 298 (Rev. 8-98)  
Prescribed by ANSI Std. Z39.18

13 separate items enclosed



2303M1A3

TP-1998-164

MEMORANDUM FOR PRR (Contractor Publication)

FROM: PROI (TI) (STINFO)

4 May 1999  
~~11 August 1998~~

SUBJECT: Authorization for Release of Technical Information, Control Number: AFRL-PR-ED-TP-1998-164  
Haddad and Lichtenhan, "Mechanical Relaxation and Microstructure of Poly(norbornyl-POSS) Copolymers"  
**Journal submission** **(Public Release)**

# Mechanical Relaxation and Microstructure of Poly(norbornyl-POSS) Copolymers.

Patrick T. Mather,<sup>a,\*</sup> Hong G. Jeon,<sup>b</sup> and A. Romo-Uribe<sup>c,#</sup>

<sup>a</sup>Air Force Research Laboratory and <sup>b</sup>Systran Corp., Materials Directorate, AFRL/MLBP, 2941 P St., Wright Patterson AFB, OH 45433-7750

Timothy S. Haddad<sup>d</sup> and Joseph D. Lichtenhan<sup>e</sup>

<sup>d</sup>Raytheon STX and <sup>e</sup>Air Force Research Laboratory, Propulsion Directorate, AFRL/PRSM, 10 E Saturn Blvd., Edwards AFB, CA 93524-7680.

**ABSTRACT:** The mechanical relaxation behavior and microstructure of a series of novel norbornyl-POSS organic-inorganic copolymers have been investigated. Furthermore, we examined the influence of weight fraction of POSS-norbornyl monomer, as well as the potential sensitivity to the seven organic corner groups present in each POSS macromer. POSS refers to the Polyhedral Oligomeric Silsesquioxane inorganic/organic macromer, which is composed of an inorganic  $\text{Si}_8\text{O}_{12}$  spherical core surrounded with seven inert organic corner groups and one reactive norbornyl moiety. It was observed that POSS copolymerization enhances the  $\alpha$ -relaxation temperature,  $T_\alpha$ , in proportion to the weight fraction of POSS-norbornyl comonomer. Interestingly, however, the magnitude of this dependence is larger for the POSS-norbornyl comonomer possessing cyclohexyl corner groups (CyPOSS) than for the copolymer with cyclopentyl corner groups (CpPOSS). While POSS copolymerization yields only slight enhancement of the tensile storage modulus for temperatures near room temperature, at temperatures lower than a strong mechanical relaxation, identified as a  $\beta$ -relaxation, and near  $T = -78^\circ\text{C}$ , there is a significant POSS-reinforcement of the storage modulus. The position of the  $\beta$ -relaxation observed in the CyPOSS series of copolymers is independent of POSS weight fraction, and the frequency dependence of this peak position yields the activation energy,  $\Delta H_\beta = 14.7 (\pm 1.25)$  kcal/mol. It is suggested that this relaxation arises from the liberation of motion of the cyclohexyl corner groups. A similar effect is observed, to some extent, for the CpPOSS copolymers, although only part of the relaxation is observed. X-ray scattering shows that the CyPOSS copolymerization preserves the amorphous character of the polynorbornene homopolymer while CpPOSS copolymerization leads to significant ordering of the POSS macromers.

#Present Address: Hoechst Research & Technology US, 86 Morris Ave., Summit, NJ 07901

## INTRODUCTION

Linear inorganic-organic hybrid polymers are receiving increasing attention, particularly in an effort to determine structure-property relationships to enable efficient materials design for specific applications. Linear hybrid polymers encompass a materials chemistry approach distinct from past efforts in sol-gel systems, which often yield crosslinking systems. Moreover, their processing characteristics differ substantially from traditional polymer processing schemes and their morphology and properties are significantly dependent on processing details. Furthermore, sol-gel hybrids have been developed largely as ceramic precursors, while linear hybrids have been developed only in part for this purpose. Perhaps stronger motivation for the study of linear hybrid polymers is the increasing level of supporting evidence for nanoscale reinforcement of mechanical properties and alteration of chain and segmental dynamics.

Polymers incorporating POSS (Polyhedral Oligomeric Silsesquioxane) macromers have been the recent focus of much research in Air Force and other laboratories.<sup>1,4,5,6-9</sup> A typical POSS macromer is a well-defined cluster represented by the formula  $P_1R_7Si_8O_{12}$  with an inorganic silica-like core ( $Si_8O_{12}$ ) surrounded by eight organic corner groups ( $P_1R_7$ ), of which seven are inert ( $R$  = cyclohexyl: CyPOSS, or  $R$  = cyclopentyl: CpPOSS) and only one is reactive. Polymerization at the single reactive "P" site results in a material that features strong potential for such applications as non-ablatives, atomic-oxygen resistance, and thermal protection (raised  $T_g$ ) of composite matrix resins. POSS has now been introduced into such thermoplastic resins as styryls, acrylics, liquid crystalline polyesters, siloxanes, and polyamides. Uniformly, it is observed that the glass transition temperature of the base resin is efficiently enhanced upon copolymerization with the associated POSS monomer.<sup>1-3,6</sup> Additionally, we have reported on the modification of rheological properties of styryl-POSS copolymers, showing evidence for retardation of chain motion and group interaction effects.<sup>7</sup> Of current interest, including the present work, is the determination of POSS modification of such solid-state properties as mechanical relaxation, fracture behavior, and abrasion resistance.

Another nanocomposite polymer system that has been extensively studied has been the organically modified clay systems intercalated or exfoliated in a polymer host, such as nylon<sup>10</sup> or poly(ethylene oxide).<sup>11</sup> These systems show a strong dependence of heat distortion temperature on

weight percentage of exfoliated clay and this feature has made such materials attractive candidates for applications featuring temperatures higher than those of the matrix polymer use temperature. The impact of clay incorporation on mechanical properties has been less studied, but it does appear that the impact properties are maintained. Additional systems relevant to the current study include polymers filled with nanometer-size silica<sup>12</sup> and polymers based on functionalized C60.<sup>13,14</sup> Studies on nanometer-scale silica have included the mechanical relaxation properties of several thermoplastics, including polyvinylacetate, polymethylmethacrylate, and poly(4-vinylpyridine). It was found that the inclusion of particles as small as 7 nm led to "double  $T_g$ " behavior which suggested that the polymer matrices consisted of two fractions, one of which was bound to the particles and possessed higher softening points, while the other fraction demonstrated bulk polymer glass transition behavior.

Previous work on physical characterization of substituted and unsubstituted polynorbornenes, the polymeric system relevant to the current study, have considered their morphology<sup>15</sup> and permeability.<sup>16</sup> In the latter study, a large increase in glass transition temperature has been reported for a trimethylsilane-substituted norbornene homopolymer<sup>16</sup> where a  $T_g$  of 113 °C, compared to  $T_g \sim 55$  °C for polynorbornene, was observed using DSC analysis.

Recently, we have developed a hybrid POSS-norbornyl monomer by connecting a POSS unit to the norbornene with an ethyl spacer (Scheme 1).<sup>17</sup> As with norbornene, this monomer can be polymerized using ring-opening metathesis polymerization (ROMP) catalysis. Additionally, we have prepared analogous diblock and triblock copolymers which will be the subject of a future report.

## EXPERIMENTAL SECTION

### ROMP Synthesis

We have prepared a series of random copolymers of norbornene/POSS-norbornene for microstructural and mechanical relaxation investigations. The POSS-norbornyl monomer was prepared by reaction of ethyl-trichlorosilane-substituted norbornene with cyclohexyl- or cyclopentyl- POSS triol in the presence of triethyl amine.<sup>17</sup> Random copolymers were all synthesized under nitrogen using the ROMP catalyst,<sup>18</sup>  $\text{Mo}(\text{C}_{10}\text{H}_{12})(\text{C}_{12}\text{H}_{17}\text{N})(\text{OC}_4\text{H}_9)_2$ ,

(purchased from Strem and used as received) in chloroform with various proportions of norbornene and the two POSS-norbornyl derivatives **1a** and **1b**. The polymerizations were designed to yield polymers with degrees of polymerization of 500 by controlling the ratio of monomers to catalyst. The reactions were terminated by addition of benzaldehyde. The polymers were precipitated and purified by adding the chloroform solutions to a large excess of methanol and collecting the precipitate. This resulted in random copolymers in yields over 90%. The synthetic route is shown in Scheme 1.

The polymers were assigned nomenclature based on the weight percentage of POSS comonomer, as well as the type of corner group present on the POSS comonomer: cyclopentyl (Cp) or cyclohexyl (Cy). For example, a random copolymer containing 10 weight percent cyclohexyl-POSS-norbornyl monomer and 90% norbornyl monomer is referred to as **10CyPN**. The polynorbornene homopolymer will be referred to as **PN**.

The molecular weights of all of the polymers, measured using static light scattering and gel-permeation chromatography, are listed in Table 1. Additionally, we list in Table 1 the weight percentages and mole percentages of POSS comonomer present in the polymers, as well as the relative *cis*- and *trans*- conformational isomers as measured using  $^1\text{H}$  NMR.

### **Molecular Characterization**

The polymers were characterized using a DAWN spectrometer from Wyatt Technologies. This spectrometer features a combination of gel-permeation chromatography (GPC) and multi-detector laser light scattering for the determination of absolute weight-average and number-average molecular weight,  $M_w$  and  $M_n$ , respectively. Characterization of the relative *cis*- and *trans*- bond content in the polymer chains was performed using  $^1\text{H}$  NMR in dilute solution with tetramethylsilane as reference. Examination of absorptions in the range of 5.1 to 5.3 ppm and 2.2 to 3.2 ppm revealed the relative content of the two tacticities resulting from the polymerizations.

### **Thermal Characterization**

The glass transition temperatures were determined using a TA Instruments differential scanning calorimeter (DSC). The temperature corresponding to the midpoint in the heat capacity step-rise is used for this purpose. Samples of mass 10 mg were used and data from the second

heating run are reported for a heating rate of  $10^{\circ}\text{C}/\text{min}$  and a nitrogen atmosphere. Thermogravimetric analysis (TGA) was carried out on a TA Instruments TGA 951 under nitrogen atmosphere at a heating rate of  $10^{\circ}\text{C}/\text{min}$ . Initial sample weights of 20 mg were employed. The decomposition-temperature,  $T_{\text{dec}}$ , was taken to be the temperature at which 5% mass loss had occurred. The residual char mass percentage,  $m_{\text{ch}}$ , was taken as the mass percentage remaining at  $T = 900^{\circ}\text{C}$ .

### Dynamic Mechanical Analysis

A Perkin Elmer DMA-7e was run in tensile mode at an oscillation frequency of 1 Hz with a static stress level of  $5 \times 10^5$  Pa and a superposed oscillatory stress of  $4 \times 10^5$  Pa. This stress controlled instrument measures the strain and phase angle difference between stress and strain. Typically the resulting strain levels ranged from 0.05% to 0.2%. Sample dimensions were typically: 5 mm long, 0.5 mm wide, and 0.2 mm thick. A gaseous helium purge and a heating rate of  $2^{\circ}\text{C}/\text{min}$  were employed. The temperature scale was calibrated with indium and the force and compliance calibrations were performed using standard weight and a clamped steel bar, respectively. Activation energy analysis requires the use of frequency scans at each temperature through the mechanical transitions of interest. Based on instrument limitations, the frequency sweeps were manually controlled and required a stabilization period of ~~two~~<sup>a</sup> minutes, per frequency, to yield reproducible results.

### X-Ray Scattering Methods

The morphological characterization was performed by using wide-angle X-ray scattering (WAXS). The samples were prepared by compression molding at a temperature above the glass-transition temperature of the apparently amorphous materials,  $T > 100^{\circ}\text{C}$ . A pressure of 15 MPa was applied to the heated compression mold for 10 minutes and the mold was then cooled under pressure to room temperature at a rate of approximately  $2^{\circ}\text{C}/\text{min}$ . A Rigaku rotating anode X-ray generator operated at 40 kV and 250 mA was employed with a Cu target and graphite monochromator. The specimens were mounted on pinhole collimator, and the diffraction patterns were recorded on a phosphoric image plate using a Statton camera. The image plates were read using a Molecular Dynamics Storm 820 image-plate reader. The image-plate processing was standardized

and the  $d$ -spacings were calibrated with silicon powder and the intensities were corrected for polarization, absorption, and geometrical factors. Intensity traces were obtained using ImageTool<sup>19</sup> software.

## RESULTS AND DISCUSSION

### Thermal Analysis.

Table 2 gives a summary of the thermal properties of both CyPOSS and CpPOSS copolymers. The  $T_g$  data, as determined from a second heating scan, along with decomposition temperature,  $T_{dec}$ , and residual char mass percentage,  $mch$ , are reported. It can be seen that the glass transition increases with increasing weight percentage of POSS, with the effect being slightly more pronounced in the CyPOSS copolymers as compared to the CpPOSS counterparts. POSS copolymerization was observed to have no significant effect on the  $T_{dec}$ , with all of the polymers being characterized by  $T_{dec} \sim 440^\circ\text{C}$ . On the other hand,  $mch$  increases substantially from 1% for PN to a maximum of 37% and 20% <sup>for</sup> 30CyPN and 30CpPN, respectively. The existence of a maxima in the  $mch$  vs.  $wp$  plot is surprising and suggests a modification of polymer morphology as well as a concomitant impact on decomposition mechanisms.

### Dynamic Mechanical Analysis

The mechanical properties of the poly(norbornene-co-norbornylCyPOSS) and poly(norbornene-co-norbornylCpPOSS) copolymers, termed %CyPN and %CpPN, respectively, were determined using dynamic mechanical testing in tensile mode over a wide range of temperatures. In order to demonstrate the salient features of our observations, we first present a comparison of the polynorbornene homopolymer, PN, with 50CyPN and 50CpPN, followed by a presentation of the data for a range of CyPN and CpPN weight percentages. Shown in Figure 1 are the storage and loss tensile moduli versus temperature for (a) PN (b) 50CyPN, and (c) 50CpPN, where the oscillation frequency is 1 Hz. Several changes to the mechanical properties are observed to result from copolymerization of 50 wt% POSS in polynorbornene. First, we observe the appearance of a strong mechanical relaxation, here termed  $\beta$  relaxation, at  $T = -78^\circ\text{C}$  in 50CyPN, which is not observed in the PN homopolymer, nor in the 50CpPN copolymer. At temperatures



below this relaxation, the storage moduli for 50CpPN and 50CyPN are quite comparable, with  $E \sim 2.0$  GPa at  $T = -140^{\circ}\text{C}$ , though with slightly different temperature dependencies. By comparison, the PN modulus at  $T = -140^{\circ}\text{C}$  is lower, with a value of  $E = 1.3$  GPa, and features a temperature dependence quite similar to the 50CpPN and distinct from 50CyPN. However, above  $T_{\beta}$ , the temperature corresponding to the  $\beta$  transition, the modulus of 50CyPN drops to values closely matching those of the PN homopolymer, while the 50CpPN storage modulus remains relatively high, not having experienced a significant mechanical relaxation. This strong dependence of the modulus profile on the POSS R-group clearly indicates that the R-group motion is the source of the  $\beta$  relaxation for the 50CyPN copolymer.

A second observation from Figure 1 is the dependence of the temperature of the primary mechanical relaxation peak in the tensile loss modulus profile, correlated with the  $\alpha$ -relaxation (defined in this work to be the peak in the loss tangent), on the amount of POSS in the copolymer. The temperature corresponding to the  $\alpha$ -relaxation is observed to increase approximately  $25^{\circ}\text{C}$  for 50CyPN over PN and, in addition, the loss modulus peak broadens significantly. 50CpPN, on the other hand exhibits a more modest increase in the loss modulus peak temperature,  $10^{\circ}\text{C}$ , though with similar peak broadening observed with the CyPOSS copolymer. Such peak broadening is sometimes associated with the presence of crystallinity in traditional linear polymers although, in PN-POSS copolymers, the magnitude of the rubber modulus and the nature of the glass-rubber transition may play a significant role.

A final feature evident in the DMA traces of Figure 1 is an alteration in the temperature dependence of the tensile moduli above  $T_{\alpha}$ , the temperature corresponding to the  $\alpha$ -relaxation, afforded by CpPOSS or CyPOSS copolymerization. While the moduli for the PN homopolymer quickly drop with temperature above  $T_{\alpha}$ , i.e., two decades over  $10^{\circ}\text{C}$ , the same drop in moduli for 50CyPN and 50CpPN takes place over a much larger temperature range of  $50^{\circ}\text{C}$ . This alteration of the moduli profiles should translate to an increase in the heat distortion temperature larger than that indicated by the increase in the  $\alpha$ -transition temperatures. It is speculated that the origin of this type of alteration in the mechanical relaxation behavior is either: (i) modification of the rheological properties of the polymer in the molten state, or (ii) morphological modification such as the

introduction of crystallinity due to POSS copolymerization. Because the shape of the relaxation peaks for  $T_\alpha$  in Figure 1(b) and 1(c) are largely symmetric, rather than biased to higher temperatures, we favor the rheological hypothesis. We will return to this point when discussing the wide-angle X-ray scattering data, presented below. Suffice to say that some precedent for the modification of polymer rheology with POSS copolymerization has been reported<sup>8</sup> and is likely to be active in this system, a subject of our current research efforts.

Figure 2 shows a comparison of the tensile storage moduli traces for the  $n$ CyPN copolymers with  $n$  values of 0, 10, 20, 30, 40, and 50 weight percent. The modest tensile modulus values are significantly affected by copolymerization with CyPOSS, showing an increase and then a decrease with increasing POSS content for temperatures between  $T_\beta$  and  $T_\alpha$ . Values of the tensile moduli near room temperature ranging from 0.75 GPa for PN to 0.92 GPa for 30CyPN. On the other hand, the tensile moduli at temperatures lower than  $T_\beta$  feature higher values on the order of 2 GPa, with a stronger dependence of modulus on CyPOSS weight percentage. In particular, the modulus values at  $T = -125^\circ\text{C}$  range from 1.19 GPa for PN to 2.11 GPa for 30CyPN. Clearly, the CyPOSS comonomer is able to reinforce the PN system, and the reinforcement is somewhat compromised above the  $\beta$ -transition. Also apparent from Figure 2 is the shift in the  $\alpha$ -transition toward increasing values with increasing weight percentage of POSS, along with a systematic decrease in the drop-off in modulus with increasing temperature as discussed above for the 50CyPN copolymer.

Figure 3 shows the temperature dependence of the tensile loss tangent for the same CyPOSS copolymers, revealing mechanical relaxation peaks similar to those of the loss modulus profile shown in Figure 1. It is seen that the  $\alpha$ -transition increases in temperature with increasing CyPOSS content, ultimately leading to the absence of a well-defined maximum for the 50CyPN copolymer. This may indicate that above  $T_\alpha$  the 50CyPN copolymer is quite rubbery, although examination of the rheological material parameters as functions of frequency have not yet been studied. Interestingly, the magnitude of the tensile loss tangent for the  $\alpha$ -transition monotonically decreases with increasing CyPOSS comonomer weight percentage. On the other hand, the peak loss tangent value for the  $\beta$ -relaxation shows a maximum value for a weight percentage of CyPOSS of 40%.

The various CyPOSS copolymers studied display strong  $\beta$ -relaxation peaks which occur at temperatures nearly independent of CyPOSS content, with  $T_\beta \approx -80^\circ\text{C}$ . Furthermore, the magnitude of the  $\beta$ -transition loss tangent peak, as mentioned above, increases with CyPOSS weight percentage to a maximum value of 0.12 for 40% CyPOSS. We have also inspected the strength of the  $\beta$ -relaxation by considering the magnitude of the step-lowering of storage modulus<sup>20</sup> as temperature is increased through the transition,

$$\Sigma = \frac{\Delta E'}{E'_0}, \quad (1)$$

and the results are plotted in Figure 4, along with the peak loss tangent data. We observe that, like the peak loss tangent, the  $\Sigma$  shows significant dependence on the weight percentage of CyPOSS with a maximum for the 40CyPN copolymer.

On inspection of the chemical structure of the CyPOSS copolymers, and noticing that the PN homopolymer features no strong  $\beta$ -relaxation, it seems plausible to assume that the relaxation results from liberation of motion of the corner cyclohexyl groups. Previously, mechanical and dielectric relaxation experiments performed on acrylic polymers containing cyclohexyl groups pendant to the polymer backbone<sup>21</sup> showed that a loss peak was also observed near  $T = -80^\circ\text{C}$  for  $f = 1$  Hz. The relaxation was attributed to the onset of a chair-chair conformational exchange motion in the cyclohexyl group, and its activation energy was measured to be 11.5 kcal/mole. For comparison with the cyclohexyl-acrylic study, and to reveal the nature of the  $\beta$ -relaxation, the frequency-dependence of  $T_\beta$ , the temperature corresponding to the peak in tensile loss tangent near  $T = -80^\circ\text{C}$ , for the 10CyPN sample was studied. The resulting Arrhenius plot is shown in Figure 5. Although the range of frequencies was limited to only several decades, the data does appear to follow an Arrhenius temperature dependence, allowing extraction of an activation energy of  $14.7 \pm 1.25$  kcal/mol. Based on the similarity in temperature and activation energy of the 10CyPN  $\beta$ -relaxation to that measured for the PMMA-Cy system, we conclude that the  $\beta$ -relaxation is attributed to the onset of motion of the cyclohexyl groups located at the corners of the CyPOSS comonomer.

The mechanical relaxation behavior of the CpPOSS copolymers has also been examined and the results are plotted in Figures 6 and 7. It is seen from the plot of tensile storage modulus versus temperature that the modulus features a strong decrease with increasing temperature for temperatures below about  $50^{\circ}\text{C}$ . This behavior follows closely that of the PN homopolymer, but with higher modulus values. The large downward slope of storage modulus for  $T < -50^{\circ}\text{C}$ , along with the lack of a significant loss tangent peak in this temperature range, suggests that a mechanical relaxation occurs in PN and CpPOSS-PN copolymers at temperatures less than  $T = -150^{\circ}\text{C}$ . Figure 6 also reveals a fairly weak dependence of tensile storage modulus on CpPOSS weight percentage, aside from an initial jump from 0.75 GPa for PN to 0.91 GPa for 10CpPN for  $T = 25^{\circ}\text{C}$ . Finally, we see from Figure 6 that the knee in the curve corresponding to the onset the glass-rubber transition occurs at temperatures which increase monotonically with the weight fraction,  $w_P$ , of CpPOSS comonomer.

The increase in the glass-rubber transition temperature with CpPOSS weight fraction is appreciated more clearly in Figure 7, where the tensile loss tangent is plotted as a function of temperature. In addition to the dependence of  $T_g$  on the weight fraction of CpPOSS, it is apparent that a dependence of the peak magnitude on POSS content is additionally present, and this will be discussed further below. Secondary relaxations are observed for temperatures near  $T = -90^{\circ}\text{C}$  superposed on a generally large loss tangent "background", although the peak magnitudes indicate weaker relaxation strengths in comparison with those of the CyPOSS copolymers (see Figure 3). While modest relaxations exist near  $T = -90^{\circ}\text{C}$  for the 10CpPN, 20CpPN, and 30 CpPN, the 40CpPN and 50CpPN copolymers deviate from this general trend and even show significantly narrow peaks centered at  $T = -30^{\circ}\text{C}$ . Remarkably, a small secondary relaxation is seen for the PN homopolymer near  $T = -30^{\circ}\text{C}$ . The source of these secondary relaxations is apparently impacted by CpPOSS copolymerization, although the details of their origin require further investigation. Nevertheless, it is apparent that the secondary relaxation temperatures for the CpPOSS copolymers are dependent on POSS weight percentage, while this is not the case for the secondary relaxation observed in the PN-CyPOSS copolymers.

Figure 8a highlights the influence of the weight percentage,  $wP$ , of CyPOSS comonomer on the tensile storage modulus of the  $n$ CyPN copolymers, at 1 Hz, as it depends on for several temperatures. At  $T = -125^{\circ}\text{C}$ , which is a temperature below the relatively strong mechanical relaxation associated with cyclohexyl groups, the modulus is found to be strongly dependent on  $wP$ , with a maximum appearing at  $wP = 30\%$  (copolymer 30CyPN). In particular, 30CyPN shows a tensile modulus 77% higher than that of the PN homopolymer. For  $wP > 30\%$ , the tensile storage modulus remains significantly higher than that of the PN homopolymer, but 15% lower than the 30CyPN sample. Near room temperature,  $T = 25^{\circ}\text{C}$ , the tensile moduli are much less dependent on  $wP$ , featuring values near 0.85 GPa. Nevertheless, a maximum in the dependence on  $wP$  still exists for the 30CyPN copolymer. For  $T = 60^{\circ}\text{C}$ , which is a temperature within the range of softening points for these copolymers, there is a clear enhancement of tensile modulus with increasing  $wP$ , the modulus value saturating with CyPOSS content at 30%. As expected, the shape of the modulus trend shown at a temperature near  $T_{\alpha}$  is quite sensitive to the precise temperature chosen, but for temperatures higher than  $T = 50^{\circ}\text{C}$  the same trend remains.

Figure 8b shows similar trends for the CpPOSS copolymers, though with some distinct differences being observed for the modulus trend at  $60^{\circ}\text{C}$ . This difference results from sensitivity of the glass transition behavior to the POSS corner-group; namely, cyclohexyl versus cyclopentyl. Additionally, the tensile modulus trend at  $-125^{\circ}\text{C}$  exhibits a local minimum for  $wP = 30\%$ , unlike the trend shown in Figure 8a for CyPOSS at the same temperature. The appearance of a local minimum in this plot seems to deviate from the general trend shown for this temperature of slightly increasing modulus with  $wP$ ; however, the observation is reproducible. As with the CyPOSS copolymers, the CpPOSS polymers show little dependence of the room temperature tensile modulus on  $wP$ . For  $T = 60^{\circ}\text{C}$ , however, the tensile modulus is found to depend strongly on  $wP$  for values larger than 20% and no saturation in this value is seen even for  $wP = 50\%$ .

Considering the dependence of  $E'$  on  $wP$  below and above the  $\beta$ -relaxation for the  $n$ CyPN copolymers as compared to the  $n$ CpPN copolymers, it is apparent that POSS-reinforcement of modulus for polynorbornene or other amorphous polymers is compromised by active motion of R-groups (present as needed for POSS assembly). The dynamic R-groups are expected to contribute

negatively to modulus, especially considering the relative amount of volume that the R-group shell occupies relative to the  $\text{Si}_8\text{O}_{12}$  core. Therefore, design of POSS monomers with smaller and less dynamic corner groups should improve the ability of POSS to reinforce the mechanical properties of thermoplastics.

The dependence of  $T_\alpha$ , as measured using the peak in the loss tangent curve, on the weight percentage of CyPOSS or CpPOSS is shown in Figure 9. Also shown with solid and dashed lines are the glass transition temperatures measured using DSC for the CpPOSS and CyPOSS copolymers, respectively. It is seen that this dependence is significant, raising  $T_\alpha$  by  $25^\circ\text{C}$  at 50 weight percent CyPOSS whereas only  $10^\circ\text{C}$  at 50 weight percent CpPOSS. Two aspects of the trends shown in Figure 9 are surprising, however. First, it is surprising that the glass transition temperature, which reflects the activation of mobility of large sections of the polymer backbone, shows significant sensitivity to the POSS corner group. In particular, why should the CyPOSS copolymers enhance  $T_g$  more efficiently than the analogous CpPOSS copolymers? One possibility may lie in the distribution of POSS comonomer in the bulk of the sample, i.e., morphological differences. This will be addressed below in the section on microstructural analysis.

Figure 10 depicts the dependence of the peak of tensile loss tangent for the  $\alpha$ -relaxation on weight percentage of POSS. In both cases, the magnitude of the loss tangent peak decreases substantially with increasing wP. Comparing the trend for the CpPOSS copolymers and the CyPOSS copolymers, the drop in the loss tangent peak value with increasing wP is more rapid for CyPOSS. Given that the loss tangent at the glass-rubber transition is a measure of the difference between the tensile modulus in glassy state and that of the rubbery state, i.e., the relaxation strength  $\Sigma$ , and the fact that the glassy modulus values for all of the POSS copolymers are comparable near  $T_\alpha$ , the uniformly observed decrease in loss tangent peak values with increasing wP indicate an increasing rubber modulus with POSS copolymerization. This indication is consistent with the data shown in Figures 2 and 6, although more extensive rheological characterization is needed to quantify the trend in rubber modulus. Nonetheless, close inspection of Figures 2 and 6 ( $T > T_\alpha$ ) reveals an increase in the negative slope of storage modulus vs. temperature plots with increasing wP.

## Microstructural Analysis

The microstructure of the polynorbornene-POSS copolymers was studied using wide-angle X-ray scattering in an effort to understand the differences between CyPOSS and CpPOSS materials observed in the dynamic mechanical analysis. The results are shown in Figure 11, where each pair of intensity traces features the CpPOSS trace vertically displaced to a position above the CyPOSS trace. In all cases, the patterns from which  $I(2\theta)$  traces were taken feature Debye Scherrer rings, indicating completely unoriented samples. The WAXS profiles shown in Figure 11 for the CyPOSS polymers show several noteworthy features. First, the PN homopolymer (trace (i)) shows a complete lack of crystallinity with a diffuse amorphous halo appearing at approximately  $18.15^\circ 2\theta$  ( $4.89 \text{ \AA}$   $d$ -spacing). Copolymerization with CyPOSS (lower traces (ii)-(vi)) leads to the gradual appearance of a second amorphous halo at a scattering angle of approximately  $7.57^\circ 2\theta$  ( $d$ -spacing of  $11.67 \text{ \AA}$ ). As the concentration of CyPOSS moieties in the copolymer increases, this peak becomes narrower in  $2\theta$  and more intense, whereas the  $18.15^\circ 2\theta$  amorphous halo decreases in intensity. This second amorphous halo, associated with the copolymerization of CyPOSS, appears at a  $d$ -spacing which is somewhat larger than that observed in the poly(4-methylstyrene-*co*-CyPOSS) system<sup>8</sup> of comparable POSS weight percentages, where a  $d$ -spacing of  $10.2 \text{ \AA}$  was observed.

The contrasting microstructural characteristics of the CpPOSS copolymers are shown in the upper WAXS scans (ii)-(vi) of Figure 11. For these copolymers, increasing the CpPOSS weight percentage in the random copolymers leads (for 40 and 50 wt. %) to a morphological change where a low angle peak, which is initially amorphous, develops into a relatively sharp peak associated with the CpPOSS groups. This crystalline peak appears at an angle which is larger than the peak position of the amorphous halo of the CyPOSS copolymers (Figure 11), at  $7.91^\circ 2\theta$  ( $11.17 \text{ \AA}$ ). In addition to this primary low-angle peak, a smaller peak appears for the 40CpPN and 50CpPN samples as a shoulder on the primary peak, at an angle of  $10.76^\circ 2\theta$  ( $8.23 \text{ \AA}$ ). This additional peak indicates further that the CpPOSS copolymers are comparatively more ordered than the CyPOSS copolymers. A similar result was observed in the styryl-CpPOSS copolymers previously studied<sup>8</sup> indicating that the steric hindrances that prevent CyPOSS copolymers from crystallizing are

somehow overcome in the CpPOSS copolymers. Another important contrasting feature apparent in Figure 11 is the shift toward larger angles (smaller  $d$ -spacings) of both the low-angle and wide-angle scattering peaks for the CpPOSS copolymers and the lack of such a shift for the CyPOSS counterparts.

The microstructural features observed in the WAXS patterns are useful to explain the observed dependence of the  $\alpha$ -relaxation temperature on the weight fraction on POSS comonomer in the polymers,  $w_P$ , and on the corner group on the POSS cage (Figure 9). In particular, Figure 11 indicated that the CpPOSS copolymers exhibit more order in the POSS-derived scattering peak while the same copolymers showed a weaker dependence of  $T_\alpha$  on  $w_P$ . We hypothesize that the difference in magnitude of the  $T_\alpha$  vs.  $w_P$  slope is attributed to the difference in "constrained volume" per POSS group. Constrained volume, a concept introduced previously to explain mechanical relaxation behavior of polymer layered silicate nanocomposites,<sup>22</sup> refers to the volume occupied by polymer segments or chains not participating in the primary  $\alpha$ -relaxation due to entropic or enthalpic factors. This difference arises from the fact that CpPOSS copolymers feature enhanced ordering of the POSS cages which, considering the pendant architecture from the synthesis, can result in local exclusion of norbornyl segments which would otherwise be part of a constrained volume shell surrounding each POSS molecule. Figure 12 shows a schematic representation for our hypothesized change in constrained volume due to POSS ordering for (a) CyPOSS copolymers and (b) CpPOSS copolymers. The light gray background represents the polynorbornene "matrix" (recognizing that in reality the POSS monomers are attached to the polynorbornene backbone), the circular white regions represent the POSS molecules, and the dark gray shells surrounding each POSS molecule or group of POSS molecules represents regions of constrained motion. This microstructural picture helps to explain our contention that POSS aggregation, even at the nanometer scale (Figure 12a), can lower the POSS-norbornene interaction volume and subsequently reduce the impact of POSS on thermal and mechanical properties. Indeed, the smaller loss tangent peak values ( $\alpha$ -relaxation) observed for the CyPOSS copolymers (Figure 10) and the WAXS analysis (Figure 11) all support this hypothesis. The validity of the proposed



microstructural picture will be tested using high resolution transmission electron microscopy (HRTEM).

## CONCLUDING REMARKS

The mechanical relaxation behavior and microstructure of norbornyl-POSS hybrid copolymers have been examined for their dependencies on the weight fraction of POSS-norbornyl monomer, and have been found to be sensitive to the seven organic corner groups present in each POSS macromer. POSS copolymerization is observed to enhance the  $\alpha$ -relaxation temperature,  $T_\alpha$ , in proportion to the weight fraction of POSS-norbornyl comonomer. However, the magnitude of this dependence is larger for POSS-norbornyl comonomer possessing cyclohexyl corner groups (CyPOSS) than for cyclopentyl corner groups (CpPOSS). While POSS copolymerization yields only slight enhancement of the tensile storage modulus for temperatures near room temperature, at temperatures lower than a strong mechanical relaxation ( $\beta$ -relaxation near  $T = -78^\circ\text{C}$ ), there is a significant POSS-reinforcement of the storage modulus. The position of the  $\beta$ -relaxation observed in the CyPOSS series of copolymers is independent of POSS weight fraction, and the frequency dependence of this peak position yields the activation energy,  $\Delta H_\beta = 14.7 (\pm 1.25)$  kcal/mol. It is concluded that this relaxation arises from the liberation of motion of the cyclohexyl corner groups. A similar effect is observed, to some extent, for the CpPOSS copolymers, although only part of the relaxation can be observed. WAXS observations show that the CyPOSS copolymerization preserves the amorphous character of the polynorbornene homopolymer while CpPOSS copolymerization leads to apparent ordering of the POSS macromers, behavior which helps to explain the influence of the POSS corner-group on thermal properties. Current efforts are focusing on direct examination of POSS copolymer morphologies using high-resolution transmission electron microscopy (HRTEM), with particular focus on the influence of mechanical deformation on the observed microstructures.

## ACKNOWLEDGMENTS.

H.G.J., A.R-U, and P.T.M. acknowledge the financial support of the U. S. Air Force Office of Scientific Research (AFOSR) and the AFRL, Materials Directorate. P.T.M. acknowledges the helpful comments of Richard A. Vaia and Kevin P. Chaffee throughout the course of this study.

## REFERENCES AND NOTES

---

- 1 Lichtenhan, J.D. et al *Macromolecules* **1993**, *26*, 2141.
- 2 Lichtenhan, J.D.; Otonari, Y.A.; and Carr, M.J. *Macromolecules* **1993**, *28*, 8435.
- 3 Haddad, T.S.; and Lichtenhan, J.D. *J. Inorg. Organomet. Polym.* **1995**, *5*, 237.
- 4 Lichtenhan, J.D. *Comm. Inorg. Chem.* **1995**, *17*, 115.
- 5 Mantz, R.A. et. al. *Chem. Mater.* **1996**, *8*, 1250.
- 6 Haddad, T.S.; Lichtenhan, J.D. *Macromolecules* **1996**, *29*, 7302.
- 7 Gilman, J.W.; Schlitzer, D.S.; and Lichtenhan, J.D. *J. Appl. Polym. Sci.* **1996**, *60*, 591.
- 8 Romo-Uribe, A.; Mather, P.T.; Haddad, T.S.; and Lichtenhan, J.D. *J. Polym. Sci. Part B: Polym. Phys.* **1998**, *36*, 1857.
- 9 Zhang, C.X. and Laine, R.M. *J. Organomet. Chem.* **1996**, *521*, 199.
- 10 Usuki, A. et al, *J. Mater. Res.* **1993**, *8*, 1179.
- 11 Vaia R.A.; Vasudevan, S.; Krawiec, W.; Scanlon, L.G., et. al. *Advanced Materials* **1995**, *7*, 154.
- 12 Tsagaropolous, G.; Eisenberg, A. *Macromolecules* **1995**, *28*, 6067.
- 13 Wignall, G.D. et. al., *Macromolecules* **1995**, *28*, 6000.
- 14 Weis, C.; Friedrich, C.; Mülhaupt, F.; and Frey, H. *Macromolecules* **1995**, *28*, 403.
- 15 Sakurai, K.; Kashiwagi, T. and Takahashi, T. *J. Appl. Polym. Sci.* **1993**, *47*, 937.
- 16 Bondar, V.I.; Kukharskii, Y.M.; Yampol'ski, Y.P.; Finkelshtein, E.S. and Makovetskii, K.L. *J. Polym. Sci. Part B: Polym. Phys.* **1993**, *31*, 1273.
- 17 Haddad, T.S.; Farris, A.R.; Mather, P.T. and Lichtenhan, J.D. *manuscript in preparation* **1998**.
- 18 See, e.g., Bazan, G.C.; Khosravi, E.; Schrock, R.R. and Feast, W.J. *J. Am. Chem. Soc.* **1990**, *112*, 8378.
- 19 ImageTool software is alpha-version software available at <http://ddsdx.uthscsa.edu/dig/itdesc.html>.

- 
- 20 McCrum, N.G.; Read, B.E. and Williams, G. *Anelastic and Dielectric Effects in Polymeric Solids*; John Wiley & Sons Ltd.: London, 1967.
- 21 Heijboer, J. *Kolloid Z.* **1960**, 171, 6.
- 22 Kojima, Y.; Usuki, A.; Kawasumi, M.; Okada, A.; Fukushima, Y.; Kurachi, T. and Kamigaito, O. *J. Mater. Res.* **1993**, 8, 1185.

## Figure and Table Captions

### Scheme 1

Synthesis of the POSS-norbornyl macromers and copolymerization with norbornene.

### Figure 1

Tensile storage (upper trace) and loss (lower trace) modulus versus temperature for a 1 Hz linear stress oscillation. (a) polynorbornene homopolymer, (b) 50CyPN, and (c) 50CpP. Heating rates of  $2^{\circ}\text{C}/\text{min}$  are used in helium atmosphere.

### Figure 2

Storage tensile modulus versus temperature for a series of CyPOSS copolymers with increasing weight percentage of CyPOSS comonomer. An oscillation frequency of 1 Hz and a heating rate of  $2^{\circ}\text{C}/\text{min}$  are used.

### Figure 3

Tensile loss tangent versus temperature for a series of CyPOSS copolymers with increasing weight percentage of CyPOSS comonomer. An oscillation frequency of 1 Hz and a heating rate of  $2^{\circ}\text{C}/\text{min}$  are used.

### Figure 4

Relaxation strength of the  $\beta$ -relaxation versus weight-percentage of CyPOSS comonomer.

### Figure 5

Arrhenius plot for determination of the activation energy of the  $\beta$ -relaxation in the 10CyPN copolymer. The natural logarithm of the inverse of the oscillation frequency is plotted versus  $1000/T$ , where  $T$  is the test temperature in  $^{\circ}\text{K}$ . From the slope we determine  $\Delta H_{\beta} = 14.7 (\pm 1.25) \text{ kcal/mol}$ .

### Figure 6

Storage tensile modulus versus temperature for a series of CpPOSS copolymers with increasing weight percentage of CpPOSS comonomer. An oscillation frequency of 1 Hz and a heating rate of  $2^{\circ}\text{C}/\text{min}$  are used.

**Figure 7**

Tensile loss tangent versus temperature for a series of CpPOSS copolymers with increasing weight percentage of CpPOSS comonomer.

**Figure 8**

(a) Tensile storage modulus versus weight percentage of CyPOSS comonomer for several temperatures: (o)  $-125^{\circ}\text{C}$ , ( $\nabla$ )  $25^{\circ}\text{C}$ , and ( $\circ$ )  $60^{\circ}\text{C}$ . (b) Tensile storage modulus versus weight percentage of CpPOSS comonomer for several temperatures: (o)  $-125^{\circ}\text{C}$ , ( $\nabla$ )  $25^{\circ}\text{C}$ , and ( $\circ$ )  $60^{\circ}\text{C}$ . An oscillation frequency of 1 Hz was used.

**Figure 9**

Glass-transition temperature versus wP for CyPOSS ( $\bullet$ ) and CpPOSS ( $\nabla$ ) comonomers. Values were obtained from the primary maximum in the loss tangent versus temperature traces. Glass transition temperatures measured using DSC are also plotted for the CyPOSS (----) and CpPOSS (—) copolymers.

**Figure 10**

Peak value of the tensile loss tangent at the glass transition versus wP for CyPOSS ( $\bullet$ ) and CpPOSS ( $\nabla$ ) comonomers.

**Figure 11**

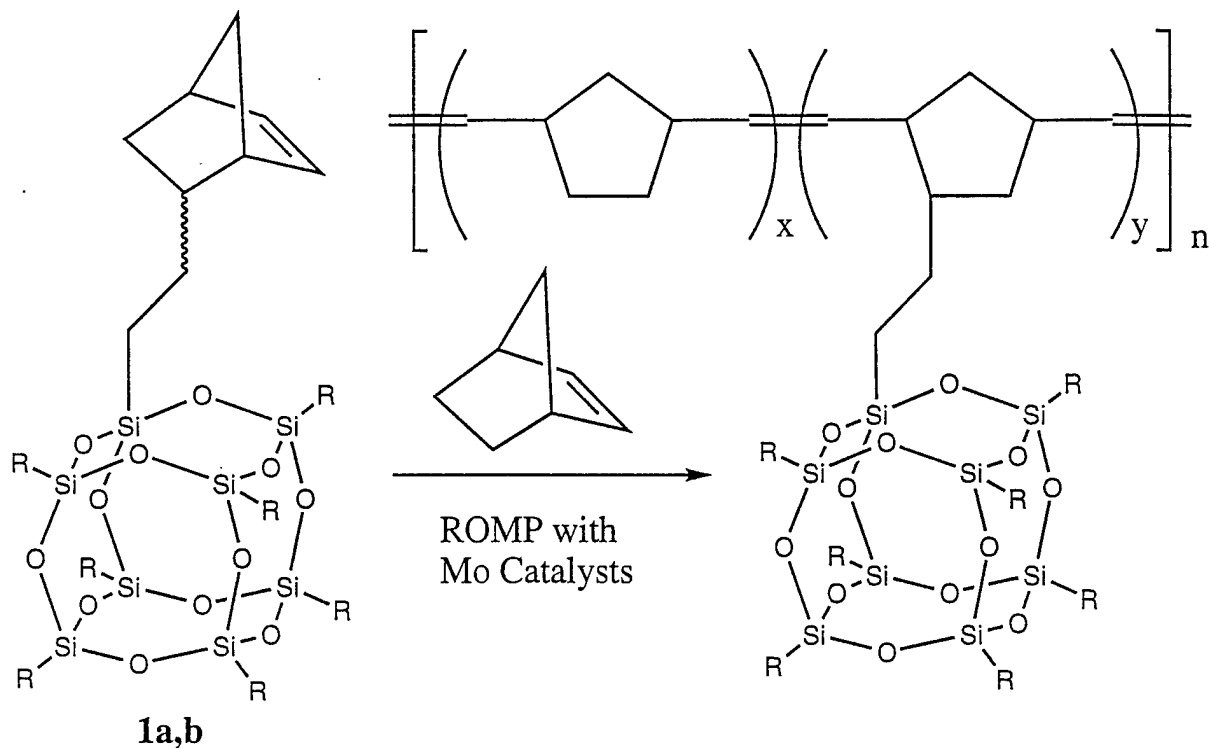
Line profiles along the radial ( $2\theta$ ) direction of wide-angle x-ray scattering (WAXS) data shown in CyPOSS (lower traces) and CpPOSS (upper traces) copolymers. Pairs of traces for various values of wP are presented: (i) 0, (ii) 10, (iii) 20, (iv) 30, (v) 40, and (vi) 50.

**Figure 12**

Schematic representation of hypothesized microstructures for (a) CyPOSS copolymers and (b) CpPOSS copolymers. The light gray background represents the polynorbornene "matrix", the circular white regions represent the POSS molecules, and the dark gray shells surrounding each POSS molecule or group of POSS molecules represents regions of constrained motion.

**Table 1**

Summary of molecular characteristics of polynorbornene-POSS copolymers.



a: R = cyclohexyl  
b: R = cyclopentyl

**R = Cyclohexyl**

| <u>Name</u> | <u>wt% POSS</u> | <u>mol% POSS</u> |
|-------------|-----------------|------------------|
| 10CyPN      | 10 %            | 0.9 %            |
| 20CyPN      | 20 %            | 2.1 %            |
| 30CyPN      | 30 %            | 3.5 %            |
| 40CyPN      | 40 %            | 5.3 %            |
| 50CyPN      | 50 %            | 7.7 %            |

**R = Cyclopentyl**

| <u>Name</u> | <u>wt% POSS</u> | <u>mol% POSS</u> |
|-------------|-----------------|------------------|
| 10CpPN      | 10 %            | 1.0 %            |
| 20CpPN      | 20 %            | 2.3 %            |
| 30CpPN      | 30 %            | 3.8 %            |
| 40CpPN      | 40 %            | 5.8 %            |
| 50CpPN      | 50 %            | 8.4 %            |

Figure 1(a); Mather et al

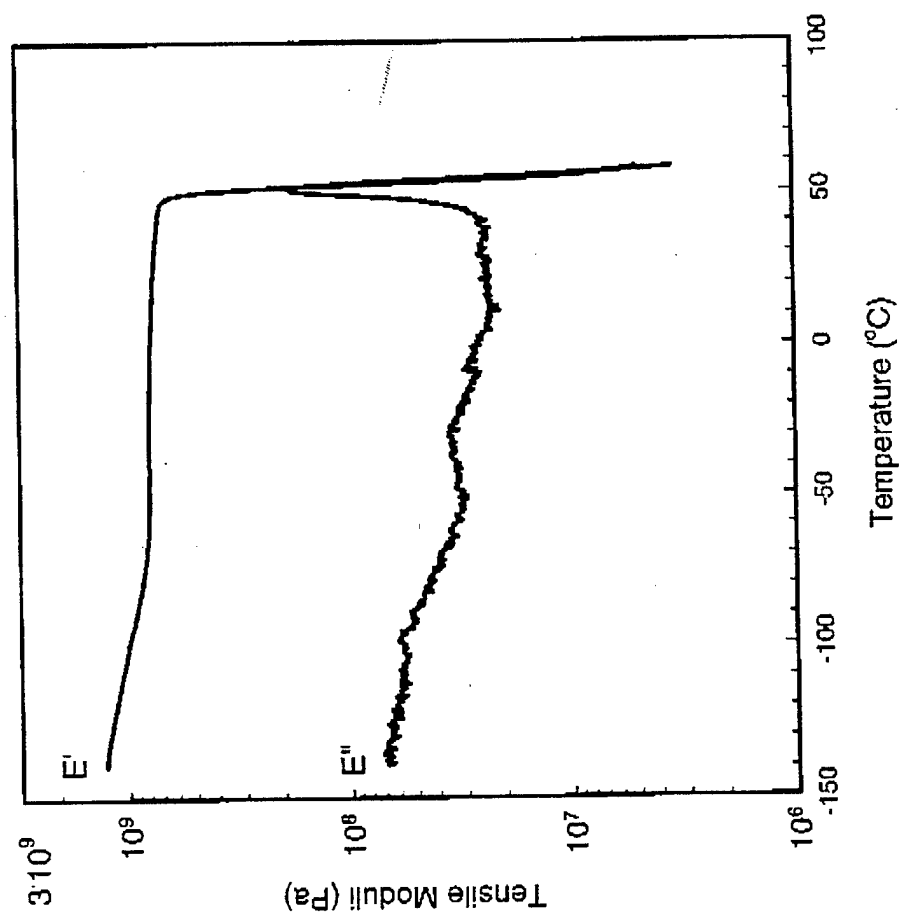


Figure 1(b); Mather et al

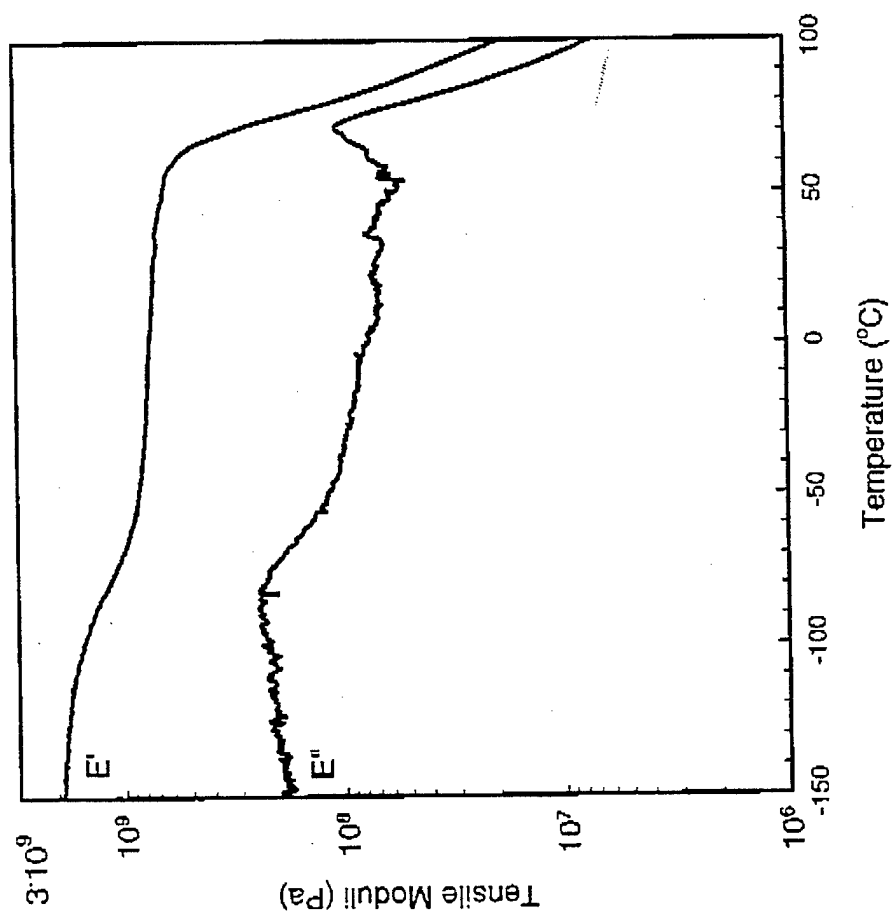




Figure 1(c); Mather et al

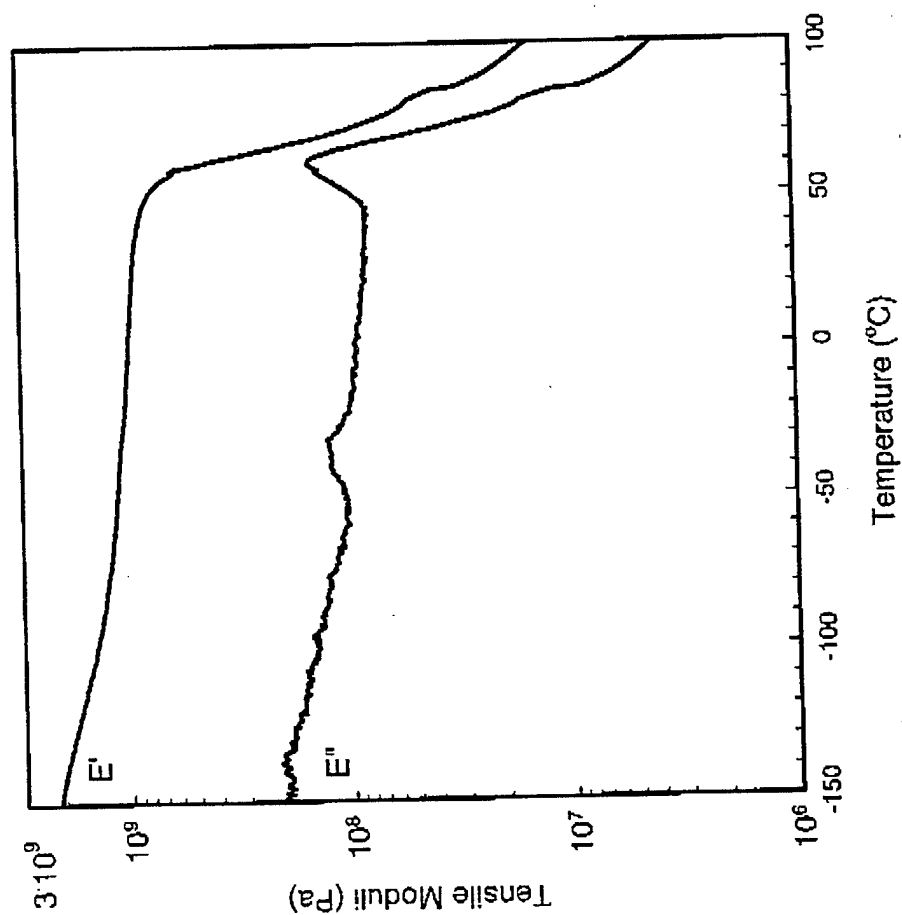


Figure 2; Mather et al

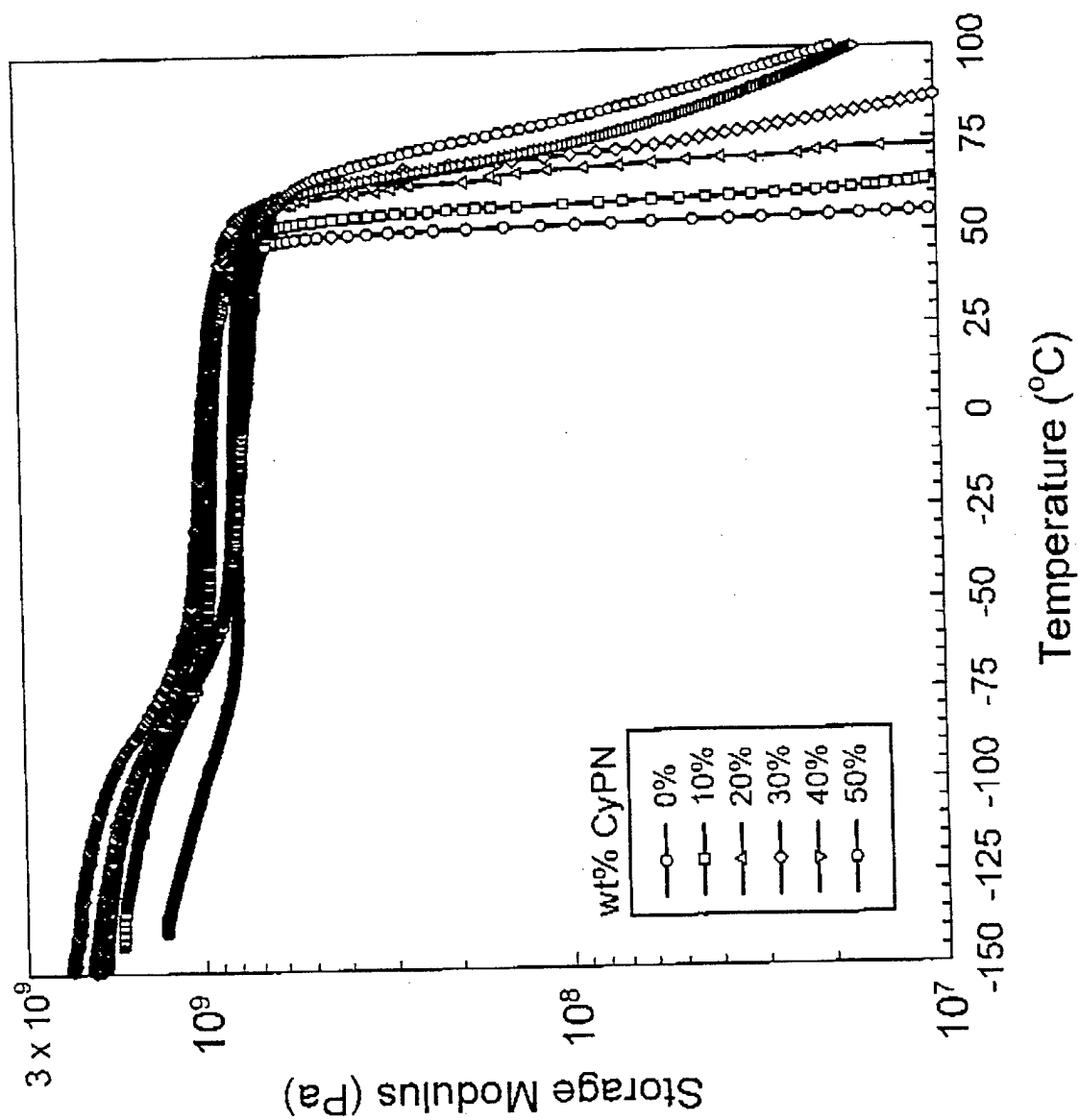


Figure 3; Mather et al

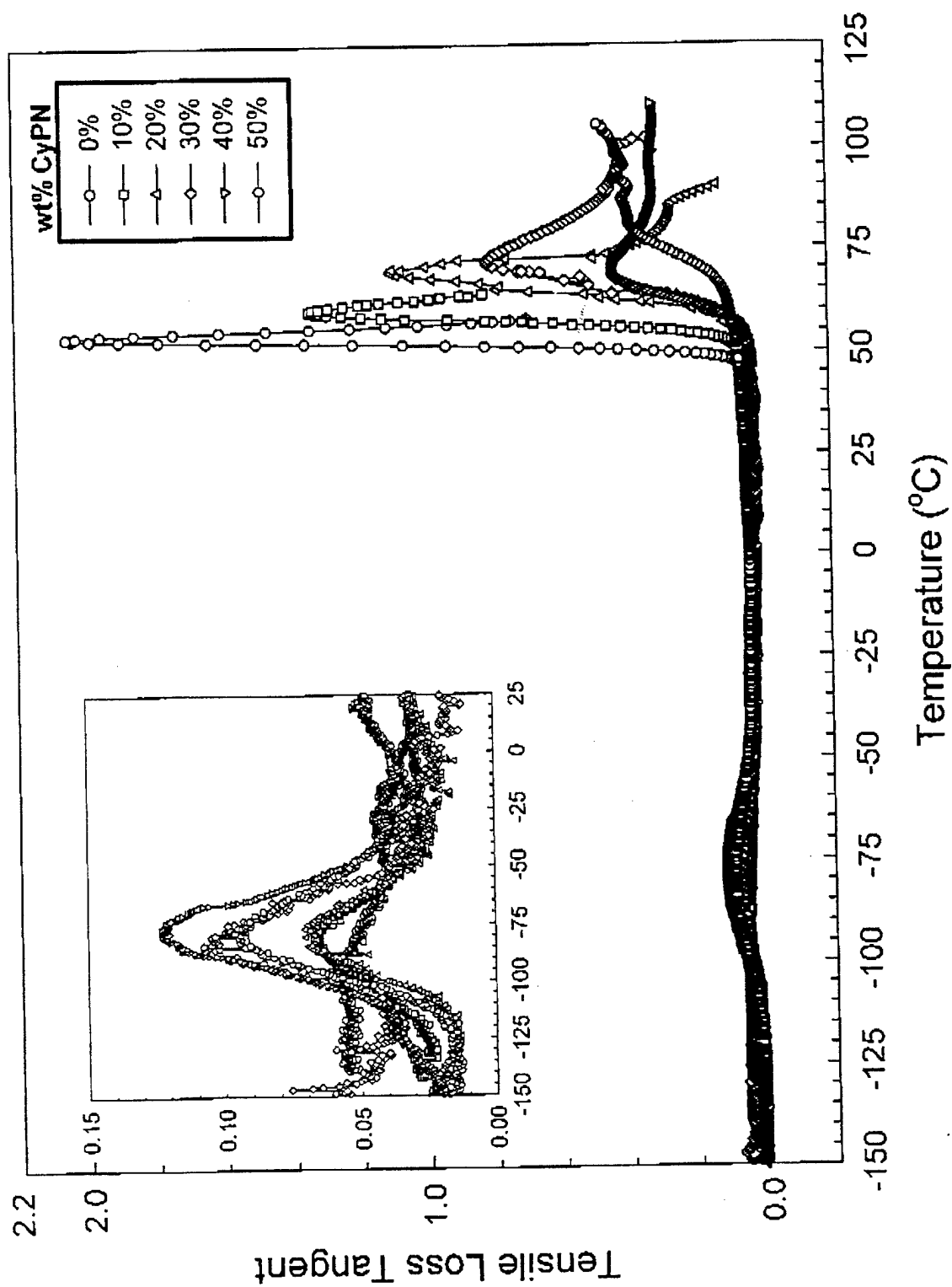


Figure 4; Mather et al

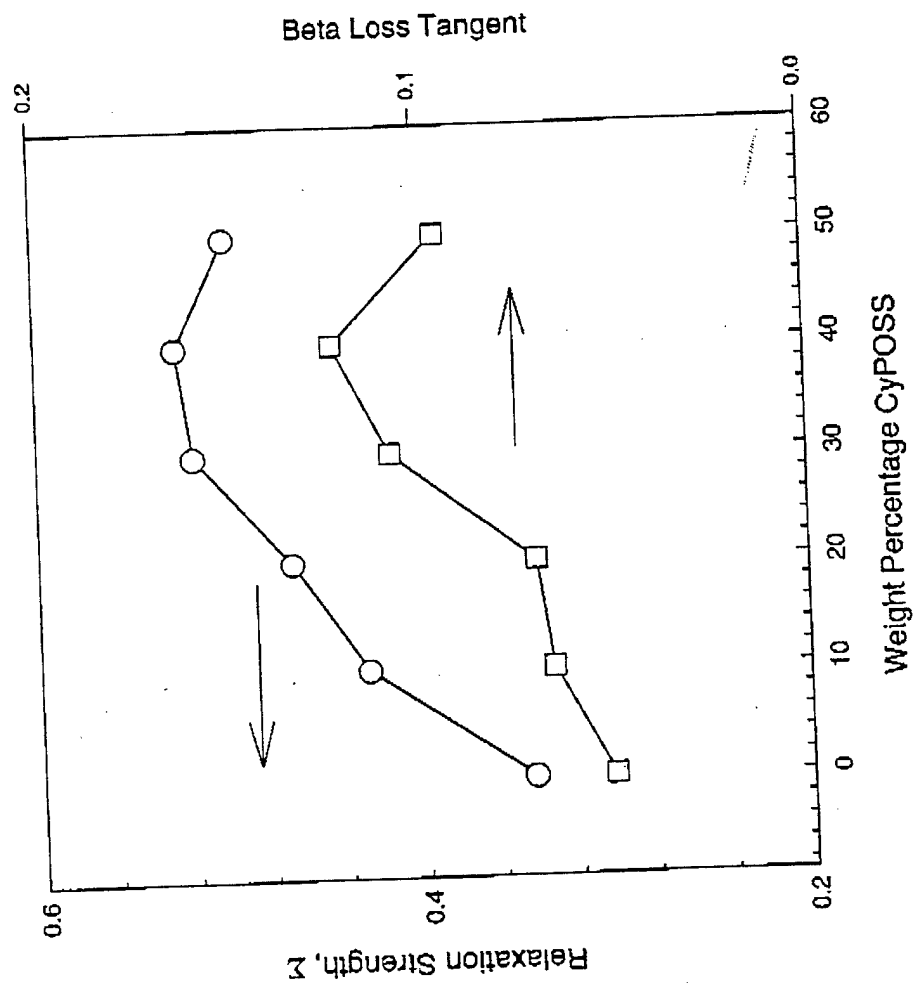


Figure 5; Mather et al

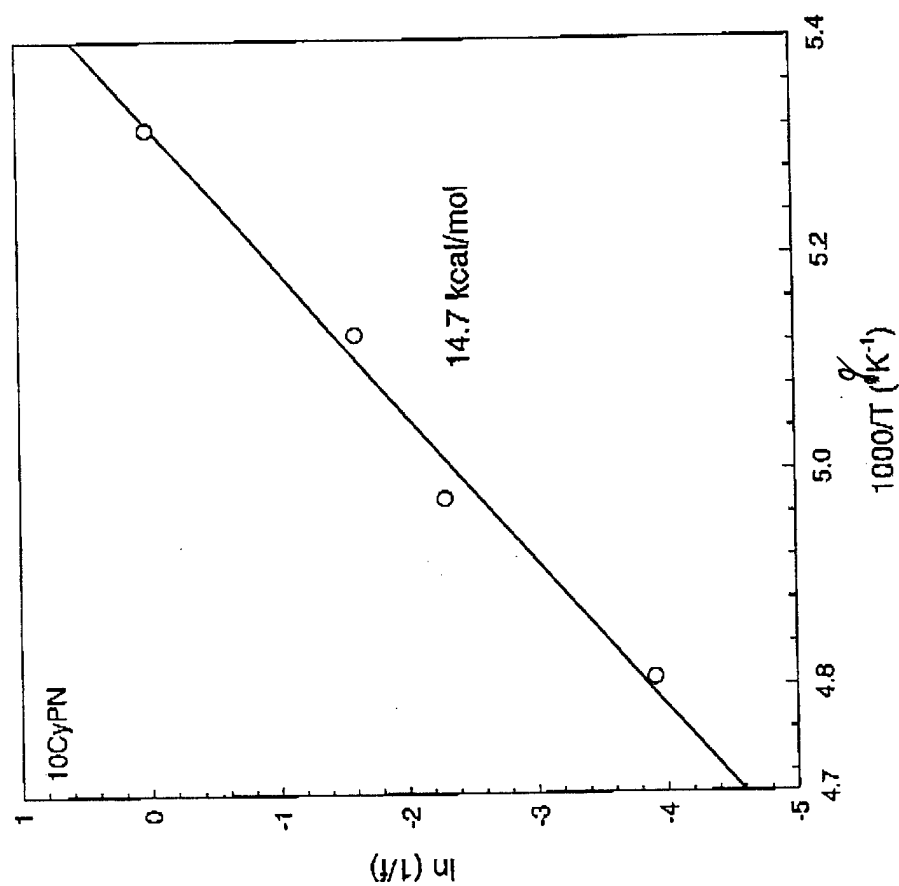


Figure 6; Mather et al

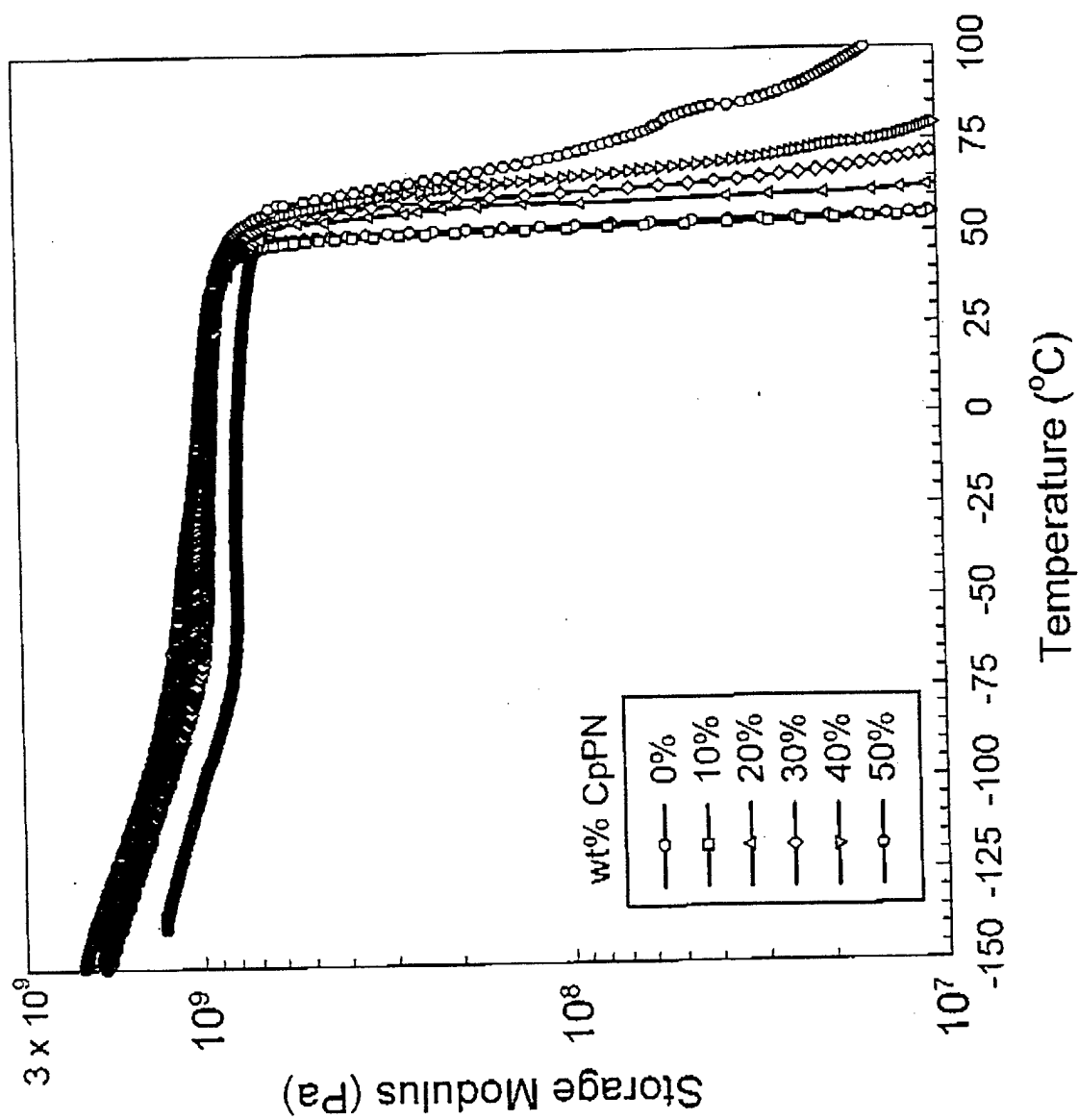


Figure 7; Mather et al

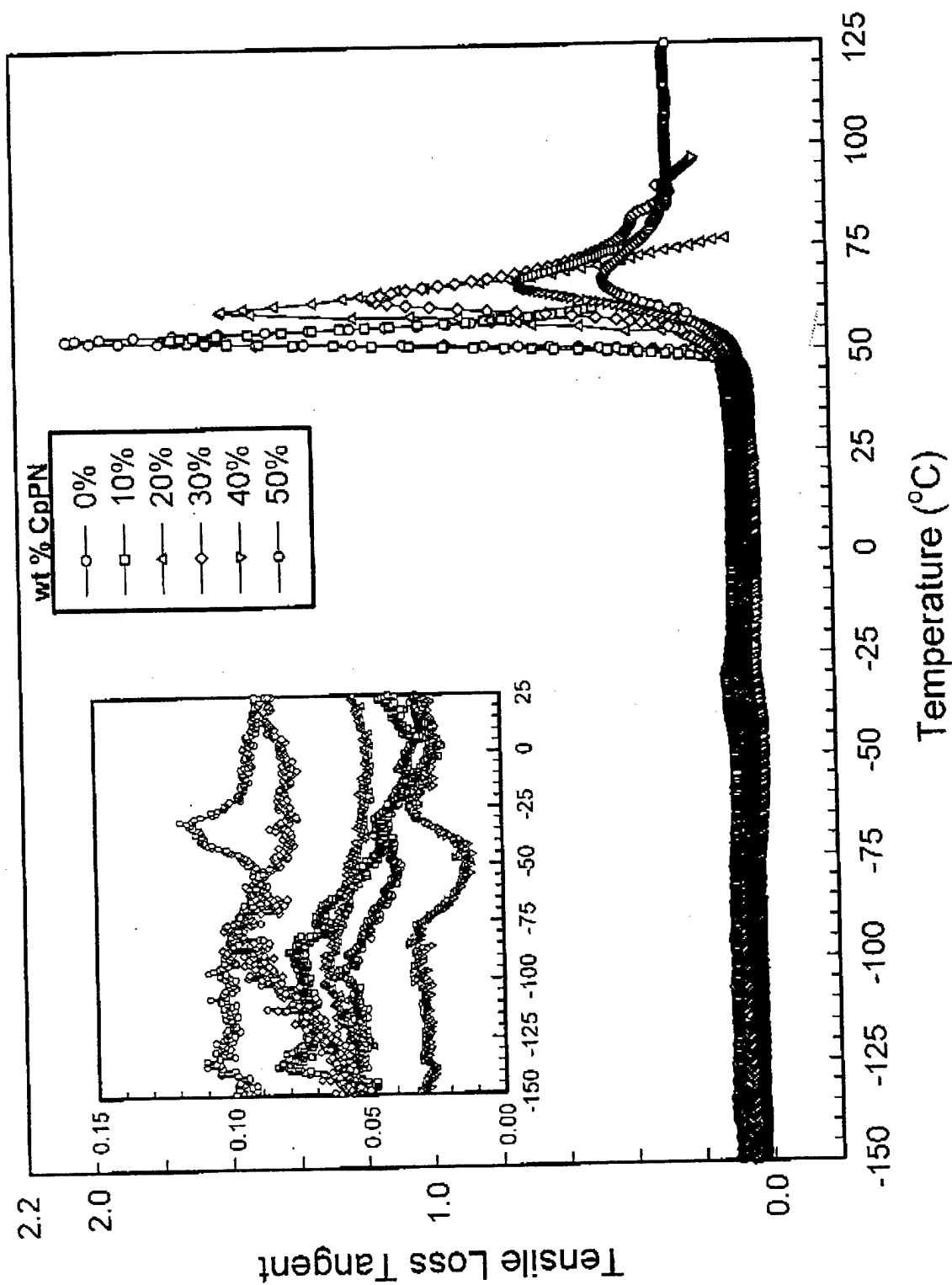


Figure 8(a); Mallet et al

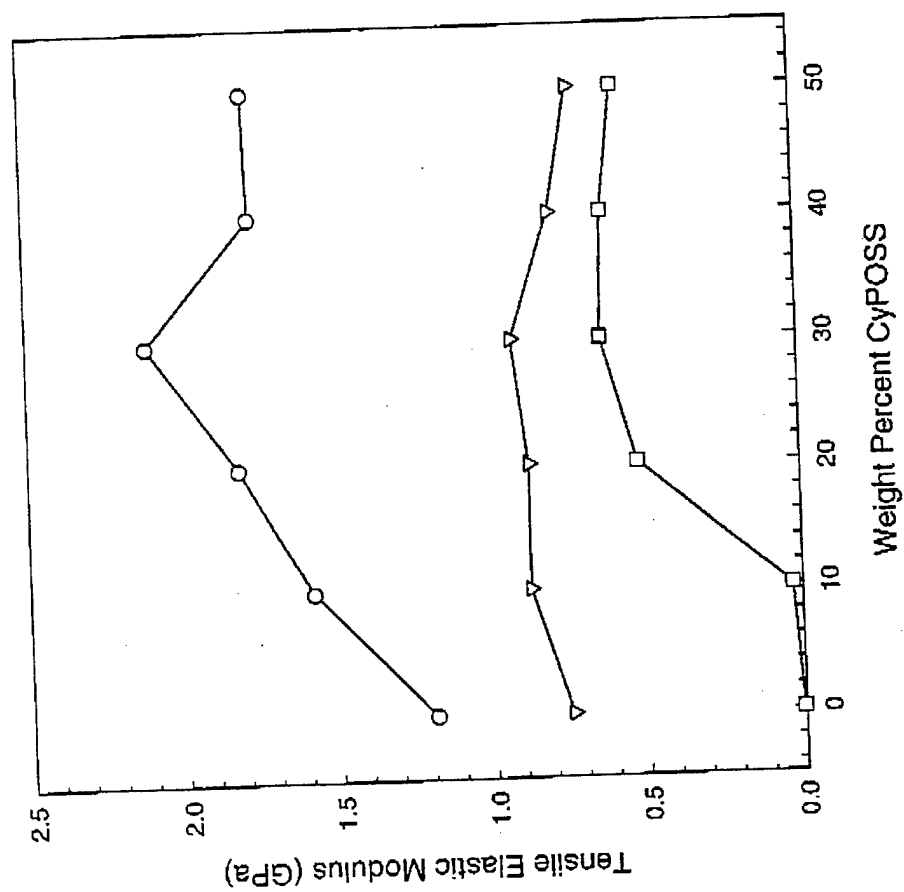




Figure 8(b); Mather et al

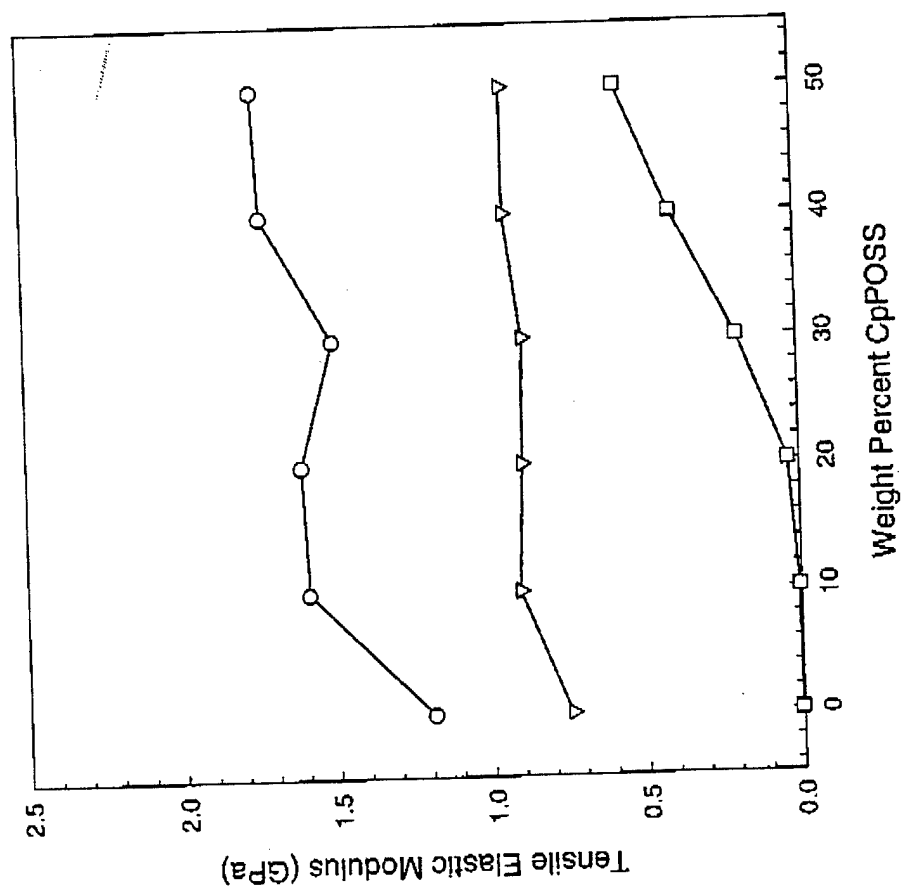


Figure 9; Mather et al

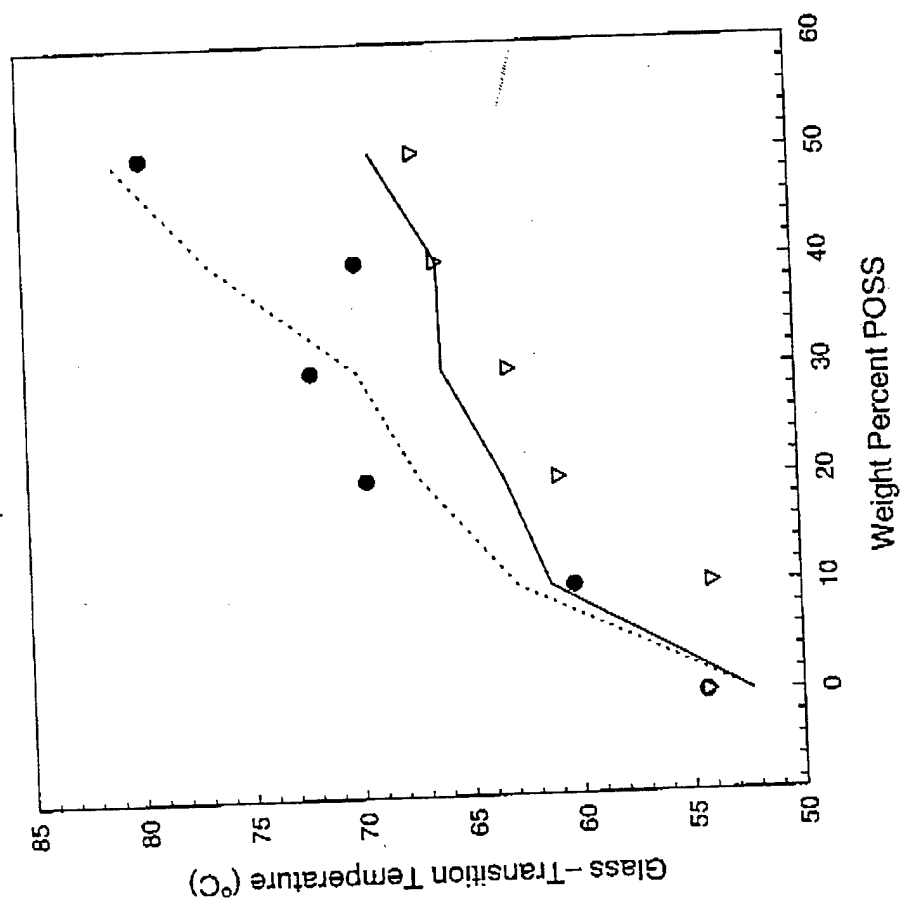


Figure 10; Mather et al

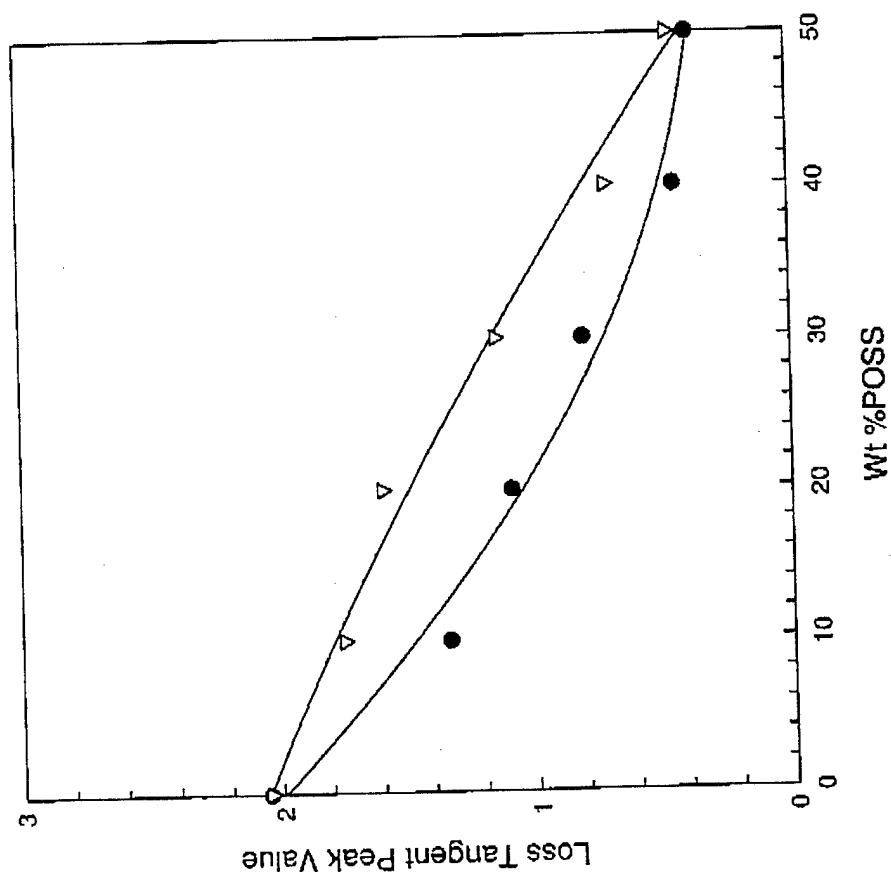


Figure 11; Mather et al

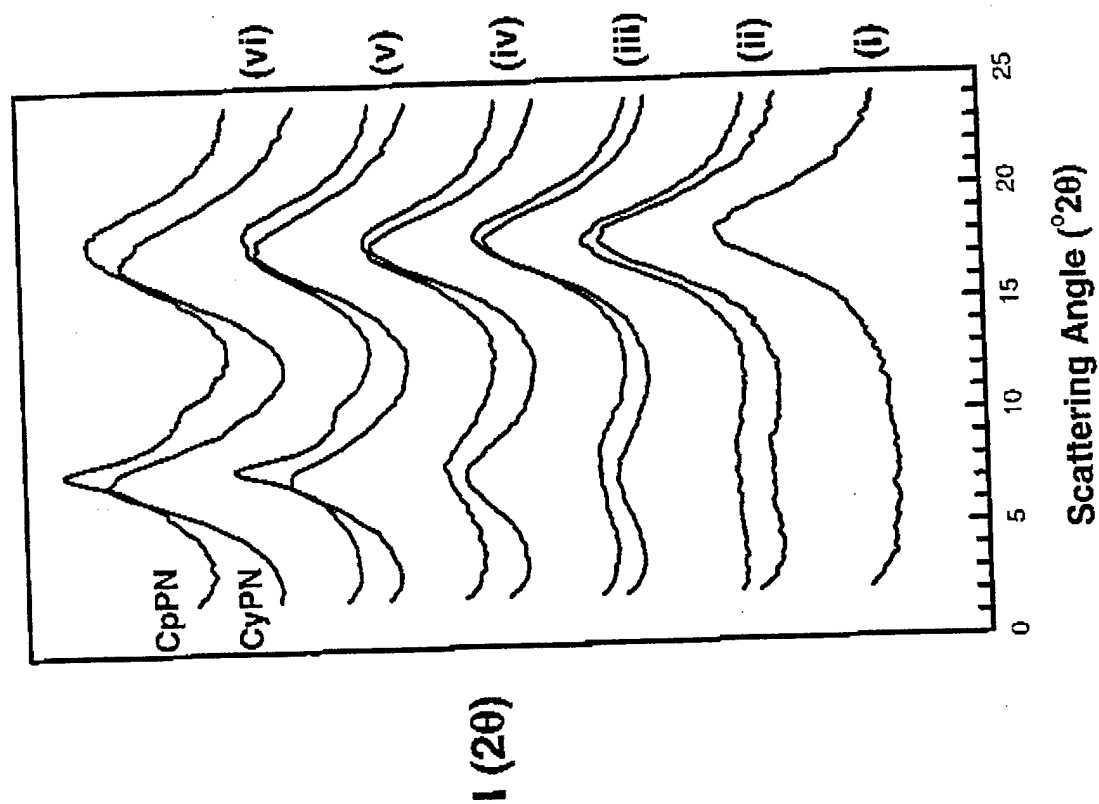


Figure 12; Mather et al

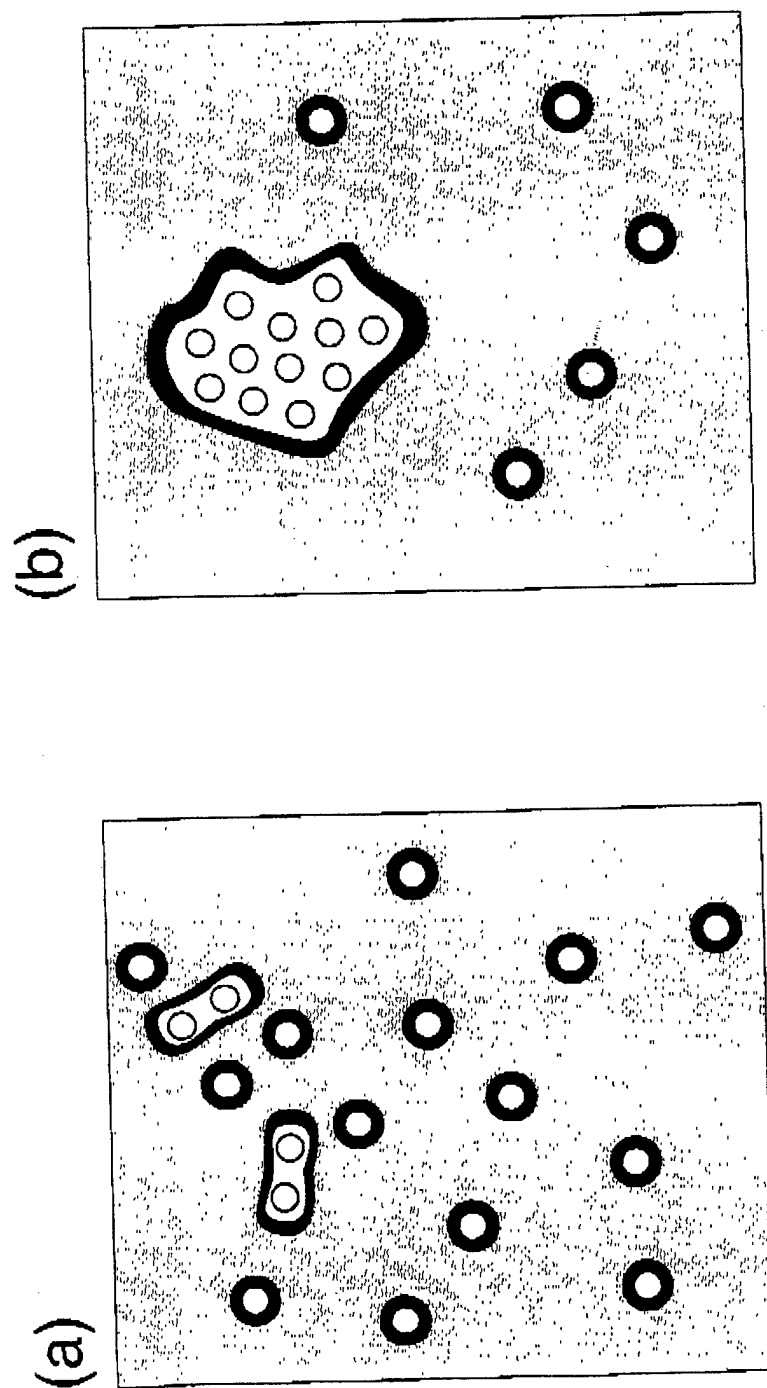


Table 1. Mather et al

| Compound | Weight %<br>POSS | Mol %<br>POSS | $M_w \cdot 10^3$<br>(g/mol) | $M_w/M_n$ | DP   | % cis |
|----------|------------------|---------------|-----------------------------|-----------|------|-------|
| PN       | 0                | 0             | 105                         | 2.94      | 381  | 60    |
| 10CyPN   | 10               | 0.9           | 75                          | 2.14      | 339  | 68    |
| 10CpPN   | 10               | 1.0           | 123                         | 2.05      | 581  | 64    |
| 20CyPN   | 20               | 2.1           | 180                         | 2.14      | 727  | 70    |
| 20CpPN   | 20               | 2.3           | 183                         | 2.51      | 633  | 68    |
| 30CyPN   | 30               | 3.5           | 220                         | 2.00      | 847  | 73    |
| 30CpPN   | 30               | 3.8           | 230                         | 2.30      | 773  | 69    |
| 40CyPN   | 40               | 5.3           | 334                         | 2.33      | 963  | 73    |
| 40CpPN   | 40               | 5.8           | 385                         | 2.57      | 1014 | 70    |
| 50CyPN   | 50               | 7.7           | 485                         | 2.85      | 983  | 71    |
| 50CpPN   | 50               | 8.4           | 740                         | 3.22      | 1337 | 69    |